Hydrol. Earth Syst. Sci. Discuss., 9, 14129–14162, 2012
www.hydrol-earth-syst-sci-discuss.net/9/14129/2012/
doi:10.5194/hessd-9-14129-2012

Hydrology and Earth System Sciences Discussions

A physically based approach for the estimation of root-zone soil moisture from surface measurements

S. Manfreda[1], L. Brocca[2], T. Moramarco[2], F. Melone[2], and J. Sheffield[3]

[1]School of Engineering, University of Basilicata, Italy
[2]Research Institute for Geo-Hydrological Protection (IRPI), National Research Council, Italy
[3]Department of Civil and Environmental Engineering, Princeton University, USA

Received: 3 October 2012 – Accepted: 11 December 2012 – Published: 20 December 2012

Correspondence to: S. Manfreda (salvatore.manfreda@unibas.it)

Published by Copernicus Publications on behalf of the European Geosciences Union.

Abstract

In the present work, we developed a new formulation for the estimation of the soil moisture in the root zone based on the measured value of soil moisture at the surface. The method sheds lights on the relationship between surface and root zone soil moisture and has applications in the use of satellite remote sensing retrievals of soil moisture. It derives from a simplified form of the soil water balance equation and provides a closed form of the relationship between the root zone and the surface soil moisture with a limited number of physically consistent parameters. The approach was first used to interpret soil moisture dynamics at the point scale using soil moisture measurements taken from the African Monsoon Multidisciplinary Analysis (AMMA) database. Thereafter it was also tested over an extended domain using modeled soil moisture data obtained from the North American Land Data Assimilation System (NLDAS). The NLDAS database provides modeled soil moisture data averaged over different depths for the conterminous US covering different climatic and physical conditions. In general, the method performed better than a traditional low pass filter and its results are found to be influenced by rainfall dynamics and also by the observed variance of soil moisture in the lower layer. The limited number of the parameters and their physical interpretation allows a direct application of the procedure to other regions.

1 Introduction

Soil moisture information is critical for weather and climate prediction, hydrological forecast applications, and watershed management (e.g. Walker and Houser, 2004; Moran et al., 2004; Manfreda and Fiorentino, 2008). However, in-situ soil moisture observations are lacking over large spatial scales. A viable alternative strategy for obtaining spatial fields of soil moisture is from satellite remote sensing, which can provide continuous and large-scale monitoring of the surface soil moisture state. These data represent an extraordinary source of information for hydrological applications, but they provide information only on near surface soil moisture. For instance, soil moisture information derived from microwave sensors is directly related to the surface soil layer (0.2–5 cm) (Gao et al., 2006; Escorihuela et al., 2010), while the volume of soil considered of interest for monitoring and forecast applications is much deeper. The description of an analytical relationship between the soil moisture at the surface and in the lower soil layers has been a significant challenge (e.g. Ragab, 1995; Puma et al., 2006; Manfreda et al., 2007; Sabater et al., 2007; Albergel et al., 2008) and warrants further study.

An important contribution was given by Wagner et al. (1999) who suggested the use of an exponential filter to convert the time series of surface measurements to a signal that is able to capture the dynamics of the lower soil layer. In the recent years, this approach has been tested with both simulated and measured data providing good results and has been extensively used to improve the description of the root-zone soil moisture in rainfall/runoff applications (e.g. Manfreda et al., 2011; Brocca et al., 2010, 2012; Matgen et al., 2012). However, a limitation of this approach is the physical interpretation of the recession constant (T) of the method. Albergel et al. (2008) investigated the correlation of the parameter, T, with soil properties and climate conditions over France, but no significant relationship was determined between T and the main soil properties (clay and sand fractions, bulk density and organic matter content).

An alternative, and increasingly useful approach is to assimilate satellite retrievals into land surface models (e.g. Reichle et al., 2002, 2004). Such an approach has benefitted from the progress made in recent years on assimilation methods and the availability of long-term records of retrievals from either microwave (e.g. Scipal et al., 2008) or thermal sensors (e.g. Crow et al., 2008) or both (e.g. Li et al., 2010). The purpose of this paper is not to define an operational approach in place of assimilation systems, but to shed light on a phenomenon of general interest. The approach proposed here represents an attempt to describe analytically the relationship between the surface soil moisture and the root zone soil moisture value using parameters that are related to the physical characteristics of the site under investigation. In this way, one may infer

HESSD
9, 14129–14162, 2012

Predicting root-zone soil moisture using surface data

S. Manfreda et al.

the soil moisture state below the surface using surface soil moisture data without the need to calibrate the parameters of the equation adopted. We test the method over west Africa using point soil moisture observations then apply it to the North American domain using model data to understand the applicability of the model over various climatic regimes. The results obtained are extremely encouraging and the methodology may represent a useful tool under some specific climatic conditions.

2 Model description

2.1 Soil Moisture Analytical Relationship (SMAR)

Several hydrological models are based on a conceptual scheme with multiple layers in order to describe the soil moisture profile. Models that make use of remote sensed data in assimilation frequently use such a representation with a surface layer of a few centimeters (e.g. Brocca et al., 2012). In the present work, the soil is assumed to be composed of two layers, one at the surface of a few centimeters (equivalent to the retrieval depth of the satellite sensor) and a second one below with a depth that may be assumed coincident with the rooting depth of vegetation (of the order of 60–150 cm). From here on, we will refer to those as the first and second layer, respectively, and we will use the subscript 1 or 2 to distinguish between their variables and parameters.

The most relevant water mass exchange between the two layers is represented by infiltration. Other processes such as lateral flow and capillary rise are assumed negligible with respect to infiltration. The challenge is to define a soil water balance equation where the infiltration term is not expressed as a function of rainfall, but of the soil moisture content in the surface soil layer. This may allow the derivation of a function of the soil moisture in one layer as a function of the other one. The water flux from the top layer can be considered significant only when the soil moisture exceeds field capacity. Assuming that during a rainfall event the soil moisture movement from the upper to the lower layer can be modeled following the Green-Ampt approach (Green-Ampt,

HESSD
9, 14129–14162, 2012

1911), one can assume that all water in the first layer above field capacity will move into the lower layer within one day. This idea was inspired by the work of Laio (2006) who proposed a model for the description of the soil moisture profile.

Under such assumptions, the infiltration flux from the top layer to the lower occurs instantaneously and is described by

$$n_1 \mathrm{Zr}_1 y(t) = n_1 \mathrm{Zr}_1 y[s_1(t), t] = n_1 \mathrm{Zr}_1 \begin{cases} (s_1(t) - s_{c1}), & s_1(t) \geq s_{c1} \\ 0, & s_1(t) < s_{c1} \end{cases} \quad (1)$$

where $y(t)$ [–] fraction of soil saturation infiltrating in the lower layer; n_1 [–] is the soil porosity of the first layer, Zr_1 [L] is the depth of the first layer, s_1 (θ_1/n_1) [–] is the relative saturation of the first layer (given by the ratio between the soil water content, θ_1, and the porosity, n_1, of the first layer), and s_{c1} [–] is the value of relative saturation at field capacity.

The above equation implies the assumption of an infinite permeability of the soil when the relative saturation reaches any value above field capacity. It is also necessary that the first layer cannot be infinitesimal, because this condition will lead to zero infiltration. Moreover, the model does not account for the saturation effect of the lower layer. It is necessary to underline that in order to avoid undesired underestimation of the infiltration the surface soil moisture value should be referred to the first 5–10 cm of soil.

Following this reasoning, the soil water balance of the second and deeper soil layer is controlled by two main factors: infiltration and soil water losses. Given the infiltration equation, we can continue with a simplified approach assuming a linear soil water loss function that includes both evapotranspiration and percolation (e.g. Porporato et al., 2004; Rodriguez-Iturbe et al., 2006). Both these processes are negligible when the soil saturation is below the wilting point. For this reason we assumed that the soil losses decrease linearly from a maximum value under well-watered conditions to 0 at the wilting point.

Defining $x = (s - s_w)/(1 - s_w)$ as the "effective" relative soil saturation and $w_0 = (1 - s_w)n\mathrm{Zr}$ the soil water storage, the soil water balance can be described by the following

HESSD
9, 14129–14162, 2012

expression:

$$(1-s_\mathrm{w})n_2\mathrm{Zr}_2\frac{\mathrm{d}x_2(t)}{\mathrm{d}t} = n_1\mathrm{Zr}_1 y(t) - V_2 x_2(t), \tag{2}$$

where s [–] represents the relative saturation of the soil, s_w [–] is the relative saturation at the wilting point, n [–] is the soil porosity, Zr [L] is the soil depth, V_2 [L T^{-1}] is the soil water loss coefficient accounting for both evapotranspiration and percolation losses and x_2 [–] is the "effective" relative soil saturation of the second soil layer.

It should be noted that this equation does not account for the high non-linearity that characterizes the soil loss function for high values of soil moisture. This simplification, along with the fact that the infiltration does not account for the saturation effect, implies some limitations in the use of such approach in humid environments.

The equation above can be simplified using normalized coefficients a and b defined as

$$a = \frac{V_2}{(1-s_\mathrm{w})n_2\mathrm{Zr}_2}, \quad b = \frac{n_1\mathrm{Zr}_1}{(1-s_\mathrm{w})n_2\mathrm{Zr}_2}. \tag{3}$$

The value of these parameters can be related directly to the ratio of the depths of the two layers and the soil water loss coefficient.

As a consequence, the soil water balance equation becomes

$$\frac{\mathrm{d}x_2(t)}{\mathrm{d}t} = b\, y(t) - a\, x_2(t). \tag{4}$$

It is interesting to note that this equation represents a generalization that also includes the case proposed by Wagner et al. (1999). Assuming an initial condition for the relative saturation $x_2(t)$ equal to zero, one may derive an analytical solution to this linear differential equation that is

$$x_2(t) = \int_0^t b\, e^{a(w-t)} y(w)\mathrm{d}w \tag{5}$$

HESSD

9, 14129–14162, 2012

Predicting root-zone soil moisture using surface data

S. Manfreda et al.

For practical applications, one may need the discrete form as well:

$$x_2(t_j) = \sum_{i=0}^{j} b\, e^{a(t_i - t_j)} y(t_i) \Delta t \tag{6}$$

Expanding Eq. (6) and assuming $\Delta t = (t_j - t_i)$, one may derive the following expression for the soil moisture in the second layer based on the time series of surface soil moisture:

$$x_2(t_j) = x_2(t_{j-1}) e^{-a\,(t_j - t_{j-1})} + b\, y(t_j)(t_j - t_{j-1}), \tag{7}$$

that may be rewritten as a function of s_2 as

$$s_2(t_j) = s_{\mathrm{w}} + (s_2(t_{j-1}) - s_{\mathrm{w}}) e^{-a\,(t_j - t_{j-1})} + (1 - s_{\mathrm{w}}) b\, y(t_j)(t_j - t_{j-1}). \tag{8}$$

The method proposed here represents a Soil Moisture Analytical Relationship (from now on we will refer to it as SMAR) between the two state variables introduced with four parameters s_{w}, s_{c1}, a, and b. All these parameters may be estimated from real data: the depth of the soil, the field capacity and the soil water losses. The last value is probably the most difficult to estimate, but is certainly a function of potential evapotranspiration and soil permeability (see Pan et al., 2003). It should be noted that the SMAR may produce values higher than 1 and that these are automatically set equal to 1.

2.2 Exponential filter

In this study, the SMAR was compared with the semi-empirical approach (also known as exponential filter) proposed by Wagner et al. (1999). This approach was derived from the soil water balance equation assuming that the changes in the soil water content are controlled by a pseudodiffusivity term that allows both positive and negative fluxes from and to the deep layer and those are all proportional to the relative change existing between the surface soil moisture and the deeper soil layer.

HESSD
9, 14129–14162, 2012

Following the same notation used since now the soil water balance equation may be written as

$$nZr\frac{ds_2}{dt} = C(s_1 - s_2) \tag{9}$$

where t is the time and C is a pseudodiffusivity coefficient that depends on the soil properties. This method assumes that the variation of the root-zone soil moisture is linearly related to the difference between the surface and root-zone soil moisture. One may immediately realize that the equation contains only one parameter that is represented by $T = nZr/C$, named the characteristic time length.

This approach leads to the development of an exponential filter that has been extensively used in remote sensing applications, but with the limitation of a physical interpretation of the parameter T. The root-zone soil moisture can be obtained by the knowledge of the surface soil moisture and a parameter T. The recursive formulation of the method relies on (Albergel et al., 2008):

$$s_2^*\left(t_j\right) = s_2^*\left(t_{j-1}\right) + K_j\left[s_1\left(t_j\right) - s_2^*\left(t_{j-1}\right)\right] \tag{10}$$

where $s_2^*\left(t_j\right)$ is the soil moisture of the second layer estimated through the exponential filter (usually defined as Soil Water Index). The gain K_j at time t_j is given by (in a recursive form):

$$K_j = \frac{K_{j-1}}{K_{j-1} + e^{-\left(\frac{t_j - t_{j-1}}{T}\right)}} \tag{11}$$

and it ranges between 0 and 1. For the initialization of this filter, K_1 and $s_2^*(t_1)$ were set to 1 and $s_2(t_1)$, respectively.

HESSD
9, 14129–14162, 2012

3 Data description

3.1 In situ observations

The proposed method (SMAR) was first tested using field measurements at various depths of three sites of the AMMA (African Monsoon Multidisciplinary Analysis) database. It is necessary to underline that the entire dataset presented in this paragraph was downloaded from the soil moisture data-base now routinely available on http://www.ipf.tuwien.ac.at/insitu/.

The AMMA programme is an international long-term collaboration to study the climatic and environmental feedback mechanisms involved in the African monsoon, and in some of its consequences on society and human health. The programme, that started in 2004, has developed a network of ground-based observation stations over Sub-saharan West Africa, and several intensive measurement campaigns (see Redelsperger et al., 2006). In particular, three meso-scale sites were implemented in Mali (de Rosnay et al., 2009), Niger (Pellarin et al., 2009a) and Benin (Pellarin et al., 2009b), providing a huge amount of information on soil moisture and many other variables. In the present paper, we focused on the point measurements taken in the meso-scale site in Niger at Banizoumbou, Wankama, and Tondikiboro.

Soil moisture data is collected over the root-zone profile at different depths starting from the surface (at 5 cm of depth) down to 135 cm of depth. For the scope of the present application, the relative saturation values at 5 cm of depth (S5) has been adopted as a reference surface measurement, while the relative saturation over the root profile has been computed averaging the soil moisture measurements below the surface layer. The resulting value of relative saturation is named S100, S130 or S135 depending on the depth of the deepest probe.

For sake of simplicity, we will first focus on Banizoumbou station that provides six soil moisture measurements over the soil profile starting from 5 cm of depth down to 100 cm. Rainfall time series and the values of relative saturation of each soil moisture probe are depicted in Fig. 1. These panels provide a complete picture of the temporal

HESSD
9, 14129–14162, 2012

dynamics of soil moisture over a period of about three years (13 May 2006–31 December 2009). Contemporary rainfall and soil saturation are available only for a period of three years, but soil moisture measurements cover a temporal window of four years.

Hourly time series have been aggregated at daily scale with the aim to evaluate the acceptability of our simplifying assumption for the present case study. A preliminary analysis on the available data was carried out to study the water losses using the time series of relative saturation in the first 5 cm of soil and the averaged value of the relative saturation of soil in the lower portion of soil (5–100 cm). These two values are named respectively S5 and S100. The time series contains some useful information that may be used in the model proposed. In particular, the loss rate can be estimated by the relative changes in the soil moisture or relative saturation from one day to the other. Plotting the relative changes of soil moisture as a function of the relative saturation of soil at different depths and for the entire volume of soil investigated provides a preliminary description of the shape assumed by the loss function in the present study case. These changes are plotted in Fig. 2 for both the soil moisture at 5 cm of depth and for the relative saturation obtained from the average of all the probes measurements (S100). These graphs have been obtained from the series of the relative changes of relative saturation of the soil at time t_j and t_{j-1} excluding all negative values and all values computed during a rainfall event. Even if in both graphs some scatter is present, a trend can be clearly detected and one may immediately realize that the assumption of a linear loss function is a reasonable one. The graphs provide a significant source of information for the description of soil moisture dynamics describing a first approximation of the soil water loss function with some scatter that may be related to rainfall not detected by the rain gauge. Moreover, the two graphs highlight the different rate of changes observed at the superficial soil layer with respect to the rate of change observed over the entire soil profile with a significant faster drying process in the surface layer. This result may be due to a higher root density in the surface layer with respect to the lower layers and also by the fact that the surface layer is more influenced by the evaporation process. The cloud of points shows that the soil water losses are negligible when the relative saturation of the soil is below 0.15. Consequently, this value can be set as wilting point for the SMAR method. Similar analysis performed on the site of Wankama and Tondikiboro allows us to identify a value for the wilting point of about 0.1.

The complete set of soil moisture measurements is given in Fig. 3 where the values of relative saturation for each probe are plotted in three different panels that provide an overview of the soil moisture dynamics at the three sites studied herein.

3.2 NLDAS modelled data

The SMAR was also tested using modelled soil moisture obtained from the North American Land Data Assimilation System (NLDAS-1) (Mitchell et al., 2004; Schaake et al., 2004). The aim of this project was to develop a retrospective data set of the land surface hydrological cycle. Simulations were carried out with four land surface models: MOSAIC, Noah, Sacramento land surface model (SAC) and Variable Infiltration Capacity (VIC). This produced a significant amount of information readily available across North America.

The analysis presented here makes use of simulations from the VIC model (Liang et al., 1994, 1996; Wood et al., 1997) for the water year October 1998 to September 1999. The VIC was run within NLDAS at 0.125° resolution. VIC describes the soil water balance using a scheme based on three soil layers, with a top layer of 10 cm and the remaining two layers have depths that vary over different regions. For the present application, we considered the averaged soil moisture in the first 10 cm and in the first 100 cm of soil that may be assumed as representative of the surface and root zone soil moisture, respectively. The reliability of the modelled soil moisture data was validated against point measurements using the Oklahoma soil moisture network (Luo et al., 2003).

The domain of interest for NLDAS is represented by the entire North America where a variety of climatic and physical conditions may be observed. The main characteristics of the area are depicted in the Fig. 4 through four panels where we reported the digital

HESSD
9, 14129–14162, 2012

elevation model (a), the map of vegetation cover (b), the map of soil porosity (that reflects the soil texture) (c), and the mean annual rainfall (d) over the studied domain. The hydrological conditions observed are extremely variable over such a large domain. In fact, strong changes may be observed in all panels and in particular in the map of mean annual rainfall.

The simulated soil moisture by the VIC model provide a huge amount of data that we have summarized in Fig. 5, where the main statistics of the relative saturation in the first 10 cm and 100 cm of soil are reported. The general pattern of the mean relative saturation as well as the variance of the process in the two soil layers is similar, but a more careful inspection of the maps reveals several differences that makes even more interesting the objective under investigation.

4 Model validation

4.1 In situ observations: AMMA database

The SMAR approach was applied to soil measurements available in West Africa and in particular for the Banizoumbou, Wankama, and Tondikiboro stations in Niger. These soil moisture measurements form an excellent database that well describes the soil moisture along the root-zone profile. According to this, we have used the surface soil moisture measurements at 5 cm depth to predict the soil moisture in the lower layer of the soil where the relative saturation is measured at various depths.

SMAR contains four parameters that can be related to physical characteristics of the soil profiles analysed. We assigned to each of those a value consistent with the physical characteristics of the site under investigation:

- parameter s_w can be estimated from the graph reported in Fig. 2a and was set equal to 0.15 for the station of Banizoumbou and equal 0.1 for the other two stations (Wankama and Tondikiboro).

HESSD
9, 14129–14162, 2012
Predicting root-zone soil moisture using surface data
S. Manfreda et al.

- The parameter s_{c1} can be assigned according to the soil texture of the site that, according to Pellarin et al. (2009), is a loamy sand. For this reason a first approximation for this parameter can be obtained from values of field capacity taken from the literature and according to those the value of s_{c1} was set equal to 0.29 (Cosby et al., 1984).
- Parameter $a = V/(n\mathrm{Zr}\ (1 - s_w))$ is computed based on the physical characteristics of the soil and assigned the following value for $n = 0.41$; Zr is the depth of the second layer of soil (that is assumed equal to 950 mm, 1250 mm and 1300 mm, respectively) and finally the value of the soil water losses was set equal to 8 mm day^{-1}. Considering that the mean annual evapotranspiration is of about 4 mm day^{-1}, the value assigned as a first guess seems a reasonable one.
- Finally the parameter b was estimated assuming the first layer of soil of 5 cm and the second one considered with a depth equal to the depth of the last probe minus 5 cm.

The results of this preliminary application are given in Fig. 6 where one can see the good performance of the method in capturing the trend of the signal of soil moisture in the lower soil layer. The graph provides a description of the application of SMAR to the three time series with the parameters assigned as described above.

The same model was also used with calibration obtained using an objective function of the RMSE between the averaged relative saturation of the lower layer of soil and the filtered time series of S5. This calibration procedure was performed for both the exponential filter (optimizing the parameter T) and the SMAR (optimizing the parameters a, b, s_w, and s_{c1}) obtaining the results given in Fig. 7. In general, the SMAR procedure produced better results in terms of correlation and RMSE, but this is not surprising considering the number of parameters of the second equation. Nevertheless, it is encouraging from our perspective that the calibration parameters are very close to those estimated based on the physical information available for the site meaning that the physical consistency of the methodology is confirmed.

HESSD
9, 14129–14162, 2012

4.2 Modeled data: NLDAS database

The second step of the present research was to test the SMAR procedure over an extended database in order to understand its limitations and extent of applicability. To this end, the VIC data set provides a great deal of information that is useful to test the SMAR under different climatic and physical conditions.

The SMAR was implemented by calibrating one (s_c) of the four parameters, and assigning a and b based on the physical characteristics of the site. The parameter s_w was set to zero for sake of simplicity. In particular, the parameter b was set equal to the ratio between the depths of the first and second layer (b is equal to 0.11). The soil water loss coefficient was computed using the mean annual potential evapotranspiration (ET_0) computed with the Blaney-Criddle formula and was set equal to $V = ET_0/(0.75 s_{c1})$, i.e. assuming that soil losses reach the value of potential evapotranspiration when the relative soil saturation is 75 % of field capacity (see Rigon et al., 2002). The parameter a was consequently computed as the ratio between V and n_2 Zr_2, where n_2 and Zr_2, where taken from the NLDAS database. Values of a computed over the NLDAS domain is significantly variable in space with a mean value around 0.0115 [day^{-1}]. In this way the model has only one parameter that needs to be calibrated (i.e. s_{c1}) and in terms of model complexity is comparable to the simple exponential filter proposed by Wagner et al. (1999).

For the present application, we compared the performances of the exponential filter proposed by Wagner et al. (1999) calibrating the parameter T and the SMAR with a calibrated value for s_{c1}. In both cases, the initial value of the filtered time series is set equal to the relative saturation averaged over the lower 100 cm (S100) layer. Calibration was carried out using six months of daily data (from October 1998 to March 1999) selecting the parameter producing the lowest root mean square error (RMSE). Calibration is carried out comparing the time series of the filtered values computed using the NLDAS data at 10 cm and the time series of the relative saturation in the first 100 cm. Performances of both the exponential filter and the SMAR have been validated

HESSD
9, 14129–14162, 2012

using the remaining six month for validation (April 1999–September 1999). Results are summarized in Figs. 8 and 9, where the maps of the R-values (Figs. 8a, c and 9a, c) and of RMSE (Figs. 8b, d and 9b, d) obtained in both cases are reported for the exponential filter (Fig. 8) and the SMAR method (Fig. 9), respectively.

Figure 8 summaries the results obtained with the exponential filter proposed by Wagner et al. (1999) using the modelled data. This figure describes the R-values as well as the RMSE obtained during the two considered periods. The comparison is extremely useful to understand that there is a significant difference between the performances observed during the calibration and the validation period. In fact, the validation displays a significant reduction of the correlation of the two time series over the entire domain considered. By contrast, the results given in Fig. 9 obtained with SMAR are particularly encouraging showing a good agreement between filtered data and S100 both in the calibration and in the validation period. In general, performances over both periods are comparable in terms of R-values and RMSE demonstrating the ability of SMAR to capture soil moisture fluctuations in the 100 cm layer. Another significant difference observed is a higher RMSE for the exponential filter that generally after its application is rescaled, then this was not surprising.

It is interesting to note that the calibrated values of s_{c1} reflect closely the pattern of soil properties, but display a range of variability that is not exactly coincident with an expected value for the field capacity. The spatial distribution of the calibrated values of s_c is given in Fig. 10 and may be compared with the map of Fig. 4c. In fact, in a portion of the domain s_{c1} tends to reach a value close to zero that in some cases correspond to areas where the R-values are very low.

An example of the application of the method is given in Fig. 11 for a point randomly chosen from sites with a correlation higher than 0.80. The graph shows the application of the newly proposed filter along with the filter proposed by Wagner et al. (1999). Both filtered time series have a correlation with S100 higher than 0.9 with the advantage that the SMAR shows a lower root mean square error, RMSE. Filtered values are named

HESSD
9, 14129–14162, 2012

S100* for the exponential filter and $S100^*_{SMAR}$ for the SMAR. Also in the present case, parameters have been calibrated only over the first 6 months of the time series.

The filtered data with SMAR depicts very well the real dynamics of soil moisture in the root-zone in many cases and this was possible using only the information of the soil moisture in the first layer. To keep our approach simple, we assumed that the parameter *a* did not change over the year. The seasonality of evapotranspiration was neglected producing a slight underestimation of S100 during winter and an overestimation during summer that is clearly visible in Fig. 11. This is a limitation that can be easily removed, but it interesting to note the physical coherence of the results and of the implication of our simplifying assumptions.

The SMAR is physically consistent, but certainly is not able to fully describe the significant differences in hydrological response found over the entire NLDAS domain, where processes related to frozen soils, interactions with phreatic surfaces, snow cover, etc, may be dominant. All these processes and many others are not considered here, nevertheless the model reproduces S100 with $R > 0.50$ over 57 % of the domain in the validation period with a RMSE of 0.071 that is certainly a satisfying result.

Further exploration of the spatial variation in the R-values (obtained in the calibration phase – Fig. 12a) with the VIC modeled S100 shows that the SMAR performances are strongly controlled by rainfall characteristics. Daily rainfall is described here through the use of two parameters usually adopted to depict daily rainfall process: the arrival rate of daily precipitation, λ, and the mean daily rainfall depth, α. The dependence on the rainfall characteristics is depicted in Fig. 12, which shows a boxplot for the correlation obtained under different combinations of rainfall characteristics. We observed that the reliability of the method increases with the value of λ when $\alpha < 6$ mm, while it decreases with the increase of λ when the mean value of the mean rainfall depth is higher than 6 mm. The correlation remains very high when the mean rainfall depth is limited between 3 mm and 6 mm for all values of λ.

Further exploring the behaviour of the SMAR, the R-values obtained were compared with several other physical characteristics and also with the main statistics of soil moisture itself. Among other facts, we observed that the variance of soil moisture in the first 100 cm is relevant for a correct description based only on surface measurements. This result may be interpreted from a physical point of view. In fact, time series of soil moisture in the lower layers of soil tends to be more stable when there is the presence of phreatic surfaces, in sites with topographic convergence for the presence of subsurface flows, in frozen soils, etc. and in all these cases the time series of soil moisture at the surface and in the lower layers of soil are more likely to be decoupled (Fig. 13).

5 Conclusions

In this paper, we introduced a new methodology for the description of soil moisture in the root zone based on the time series of surface data. The SMAR has a physically consistent structure with parameters that may be estimated from the physical characteristics of the site under investigation. Results obtained using as much available physical information as possible provided good results.

The methodology was also applied using measured and modelled soil moisture providing prediction of the relative saturation over two significantly different spatial scales. Regarding the point measurements, the SMAR has been applied using available information in order to infer parameter values. A preliminary application carried out without the need of any calibration provided a satisfying result both in terms of R-values and RMSE.

The model showed high reliability when applied over the conterminous US (plus northern Mexico and southern Canada). Its performance is highly influence by rainfall characteristics and the dynamics of soil moisture in the lower layers. In fact, the analysis highlighted a significant increase in the performances when the time variability of the soil moisture observed in the deeper layer increases. The skill of the method is therefore encouraging and there is potential to use the method to derive root-zone soil moisture from satellite retrievals.

HESSD
9, 14129–14162, 2012

The proposed method may be improved by including a soil loss function that accounts for the non-linearity of this process. This step is straightforward, but will incorporate a significant number of additional parameters in the proposed relationship, while in the present form the equation provides an interesting descriptive functional relationship between to variable of extreme interest.

References

Albergel, C., Rüdiger, C., Pellarin, T., Calvet, J.-C., Fritz, N., Froissard, F., Suquia, D., Petitpa, A., Piguet, B., and Martin, E.: From near-surface to root-zone soil moisture using an exponential filter: an assessment of the method based on in-situ observations and model simulations, Hydrol. Earth Syst. Sci., 12, 1323–1337, doi:10.5194/hess-12-1323-2008, 2008.

Brocca, L., Melone, F., Moramarco, T., Wagner, W., Naeimi, V., Bartalis, Z., and Hasenauer, S.: Improving runoff prediction through the assimilation of the ASCAT soil moisture product, Hydrol. Earth Syst. Sci., 14, 1881–1893, doi:10.5194/hess-14-1881-2010, 2010.

Brocca, L., Moramarco, T., Melone, F., Wagner, W., Hasenauer, S., and Hahn, S.: Assimilation of surface and root-zone ASCAT soil moisture products into rainfall-runoff modelling, IEEE T. Geosci. Remote, 50, 2542–2555, 2012.

Cosby, B. J., Hornberger, G. M., Clapp, R. B. and Ginn, T. R.: A Statistical Exploration of the Relationships of Soil Moisture Characteristics to the Physical Properties of Soils, Water Resour. Res., 20, 682–690, 1984.

Crow, W. T., Kustas, W. P., and Prueger, J. H.: Monitoring root-zone soil moisture through the assimilation of a thermal remote sensing-based soil moisture proxy into a water balance model, Remote Sens. Environ., 112, 1268–1281, 2008.

de Rosnay, P., Gruhier, C., Timouk, F., Baup, F., Mougin, E., Hiernaux, P., Kergoat, L., and LeDantec, V.: Multi-scale soil moisture measurements at the Gourma meso-scale site in Mali, J. Hydrol., 375, 241–252, 2009.

Escorihuela, M., Chanzy, A., Wigneron, J., and Kerr, Y.: Effective soil moisture sampling depth of L-band radiometry: a case study, Remote Sens. Environ., 114, 995–1001, 2010.

Gao, H., Wood, E. F., Jackson, T. J., Drusch, M., Bindlish, R.: Using TRMM/TMI to Retrieve Surface Soil Moisture over the Southern United States from 1998 to 2002, J. Hydrometeorol., 7, 23–38, 2006.

HESSD

9, 14129–14162, 2012

Predicting root-zone soil moisture using surface data

S. Manfreda et al.

Green, W. H. and Ampt, G.: Studies of soil physics, part I – the flow of air and water through soils, J. Agr. Sci., 4, 1–24, 1911.
Laio, F.: A vertically extended stochastic model of soil moisture in the root zone, Water Resour. Res., 42, W02406, doi:10.1029/2005WR004502, 2006.
Liang, X., Lettenmaier, D. P., Wood, E. F., Burges, S. J.: A simple hydrologically based model of land surface water and energy fluxes for GCMs, J. Geophys. Res., 99, 14415–14428, 1994.
Liang, X., Lettenmaier, D. P., Wood, E. F.: One-dimensional statistical dynamic representation of subgrid spatial variability of precipitation in the two-layer variable infiltration capacity model, J. Geophys. Res., 101, 21403–21422, 1996.
Li, F., Crow, W. T., and Kustas, W. P.: Towards the estimation of root-zone soil moisture via the simultaneous assimilation of thermal and microwave soil moisture retrievals, Adv. Water Resour., 33, 201–214, 2010.
Luo, L., Robock, A., Mitchell, K. E., Houser, P. R., Wood, E. F., Schaake, J. C., Lohmann, D., Cosgrove, B., Wen, F., Sheffield, J., Duan, Q., Higgins, W., Pinker, R. T., and Dan Tarpley, J.: Validation of the North American Land Data Assimilation System (NLDAS) retrospective forcing over the southern Great Plains, J. Geophys. Res., 108, 8843, doi:10.1029/2002JD003246, 2003.
Manfreda, S. and Fiorentino, M.: A stochastic approach for the description of the water balance dynamics in a river basin, Hydrol. Earth Syst. Sci., 12, 1189–1200, doi:10.5194/hess-12-1189-2008, 2008.
Manfreda, S., McCabe, M., Wood, E. F., Fiorentino, M. and Rodriguez-Iturbe, I.: Spatial Patterns of Soil Moisture from Distributed Modeling, Adv. Water Resour., 30, 2145–2150, 2007.
Manfreda, S., Lacava, T., Onorati, B., Pergola, N., Di Leo, M., Margiotta, M. R., and Tramutoli, V.: On the use of AMSU-based products for the description of soil water content at basin scale, Hydrol. Earth Syst. Sci., 15, 2839–2852, doi:10.5194/hess-15-2839-2011, 2011.
Matgen, P., Heitz, S., Hasenauer, S., Hissler, C., Brocca, L., Hoffmann, L., Wagner, W., and Savenije, H. H. G.: On the potential of METOP ASCAT-derived soil wetness indices as a new aperture for hydrological monitoring and prediction: a field evaluation over Luxembourg, Hydrol. Process., 26, 2346–2359, 2012.
Mitchell, K. E., Lohmann, D., Houser, P. R., Wood, E. F., Schaake, J. C., Robock, A., Cosgrove, B. A., Sheffield, J., Duan, Q., Luo, L., Higgins, R. W., Pinker, R. T., Tarpley, J. D., Lettenmaier, D. P., Marshall, C. H., Entin, J. K., Pan, M., Shi, W., Koren, V., Meng, J., Ramsay, B. H., and Bailey, A. A.: The Multi-institution North American Land Data Assimilation System (NLDAS):

Utilizing multiple GCIP products and partners in a continental distributed hydrological modeling system, J. Geophys. Res., 109, D07S90, doi:10.1029/2003JD003823, 2004.
Moran, M. S., Peters-Lidard, C. D., and Stephen McElroy, J. M. W.: Estimating soil moisture at the watershed scale with satellite-based radar and land surface models, Can. J. Remote Sens., 30, 805–826, 2004.
Pan, F., Peters-Lidard, C. D., and Sale, M. J.: An analytical method for predicting surface soil moisture from rainfall observations, Water Resour. Res., 39, 1314, doi:10.1029/2003WR002142, 2003.
Pellarin, T., Laurent, J. P., Cappelaere, B., Decharme B., Descroix, L., and Ramier, D.: Hydrological modelling and associated microwave emission of a semi-arid region in South-western Niger, J. Hydrol., 375, 262–272, 2009a.
Pellarin, T., Tran, T., Cohard, J.-M., Galle, S., Laurent, J.-P., de Rosnay, P., and Vischel, T.: Soil moisture mapping over West Africa with a 30-min temporal resolution using AMSR-E observations and a satellite-based rainfall product, Hydrol. Earth Syst. Sci., 13, 1887–1896, doi:10.5194/hess-13-1887-2009, 2009b.
Porporato, A., Daly, E., and Rodriguez-Iturbe, I.: Soil water balance and ecosystem response to climate change, Am. Nat., 164, 625–632, 2004.
Puma, M. J., Celia, M. A., Rodriguez-Iturbe, I., and Guswa, A. J.: Functional relationship to describe temporal statistics of soil moisture averaged over different depths, Adv. Water Resour., 28, 553–66, 2005.
Ragab, R.: Towards a continuous operational system to estimate the root zone soil moisture from intermittent remotely sensed surface moisture, J. Hydrol., 173, 1–25, 1995.
Redelsperger, J.-L., Thorncroft, C. D., Diedhiou, A., Lebel, T., Parker, D., and Polcher, J.: African Monsoon Multidisciplinary Analysis: An International Research Project and Field Campaign, Bull. Am. Meteorol. Soc., 87, 1739–1746, 2006.
Reichle, R., McLaughlin, D., and Entekhabi, D.: Hydrologic data assimilation with the ensemble kalman filter, Mon. Weather Rev., 130, 103–114, 2002.
Reichle, R., Koster, R., Dong, J., and Berg, A.: Global soil moisture from satellite observations, land surface models, and ground data: implications for data assimilation, J. Hydrometeorol., 5, 430–442, 2004.
Rigon, R., Bertoldi, G., and Over, T. M.: GEOTOP: un modello del ciclo idrologico, Proceedings of 28th Convegno Nazionale di Idraulica e Costruzioni Idrauliche, 1, 303–312, 2002.

HESSD
9, 14129–14162, 2012

Predicting root-zone soil moisture using surface data

S. Manfreda et al.

Sabater, J. M., Jarlan, L., Calvet, J. C., Bouyssel, F., and De Rosnay, P.: From Near-Surface to Root-Zone Soil Moisture Using Different Assimilation Techniques, J. Hydrometeorol., 8, 194–206, 2007.

Scipal, K., Drusch, M., and Wagner, W.: Assimilation of a ERS scatterometer derived soil moisture index in the ECMWF numerical weather prediction system, Adv. Water Resour., 31, 1101–1112, 2008.

Schaake, J. C., Duan, Q., Koren, V., Mitchell, K. E., Houser, P. R., Wood, E. F., Robock, A., Lettenmaier, D. P., Lohmann, D., Cosgrove, B., Sheffield, J., Luo, L., Wayne Higgins, R., Pinker, R. T., and Dan Tarpley, J.: An intercomparison of soil moisture fields in the North American Land Data Assimilation System (NLDAS), J. Geophys. Res., 109, D01S90, doi:10.1029/2002JD003309, 2004.

Wagner, W., Lemoine, G., and Rott, H.: A method for estimating soil moisture from ERS scatterometer and soil data, Remote Sens. Environ., 70, 191–207, 1999.

Walker, J. P. and Houser, P. R.: Requirements of a global near-surface soil moisture satellite mission: accuracy, repeat time, and spatial resolution, Adv. Water Resour., 27, 785–801, 2004.

Wood, E. F., Lettenmaier, D. P., Liang, X., Nijssen, B., and Wetzel, S. W.: Hydrological modeling of continental-scale basins, Annu. Rev. Earth Pl. Sc., 25, 279–300, 1997.

HESSD

9, 14129–14162, 2012

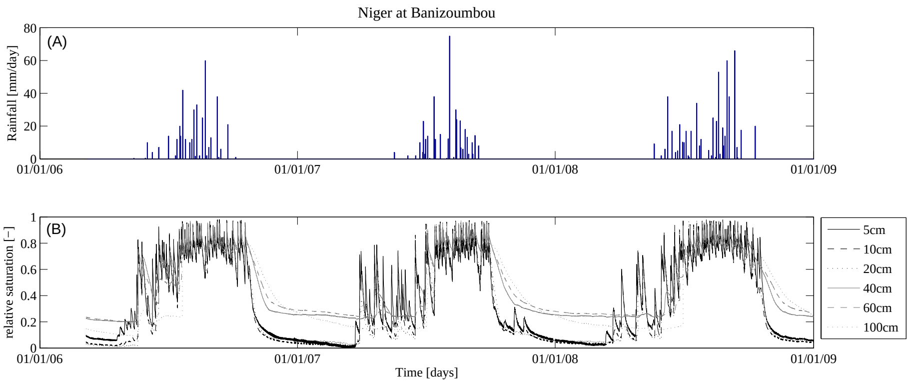

Fig. 1. Field measurements taken from the AMMA database relative to the station of Banizoumbou, in Niger: **(A)** daily rainfall time series for the period 13 May 2006–31 December 2009 and **(B)** point measurements at 5 cm, 10 cm, 20 cm, 40 cm, 60 cm, and 100 cm of depth.

HESSD
9, 14129–14162, 2012

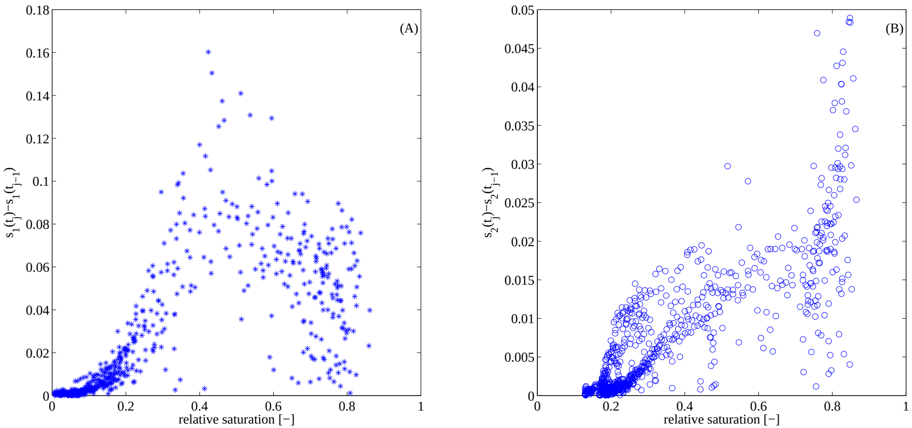

Fig. 2. Relative changes of the soil saturation as a function of the relative saturation of the soil in the first **(A)** and second layer **(B)**.

HESSD
9, 14129–14162, 2012

Predicting root-zone soil moisture using surface data

S. Manfreda et al.

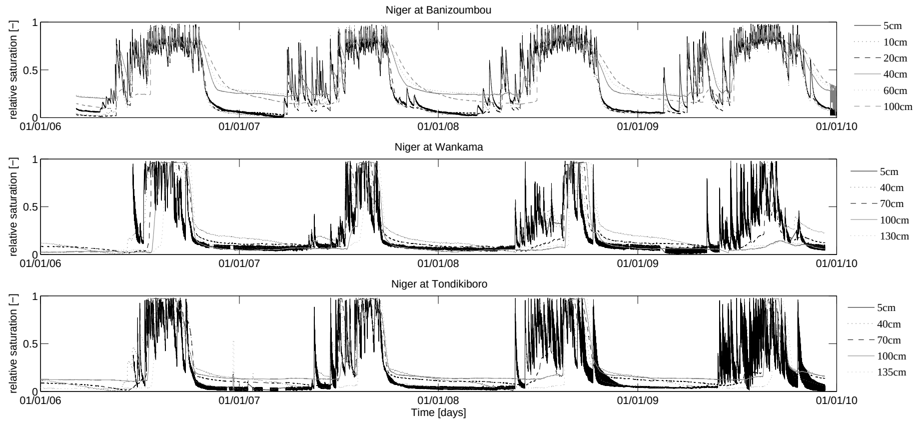

Fig. 3. Time series of the point measurements of the relative saturation of soil at the tree stations of the AMMA network: Banizoumbou, Wankama, and Tondikiboro in Niger. Point measurements provide a good description of the soil moisture variations along the soil profile with 6 or 5 measurements at different depths ranging from 5 cm down to 100–135 cm. Data refers to the period 13 May 2006–31 December 2010.

HESSD
9, 14129–14162, 2012

Title Page
Abstract | Introduction
Conclusions | References
Tables | Figures
◀| |▶
◀ ▶
Back | Close
Full Screen / Esc
Printer-friendly Version
Interactive Discussion

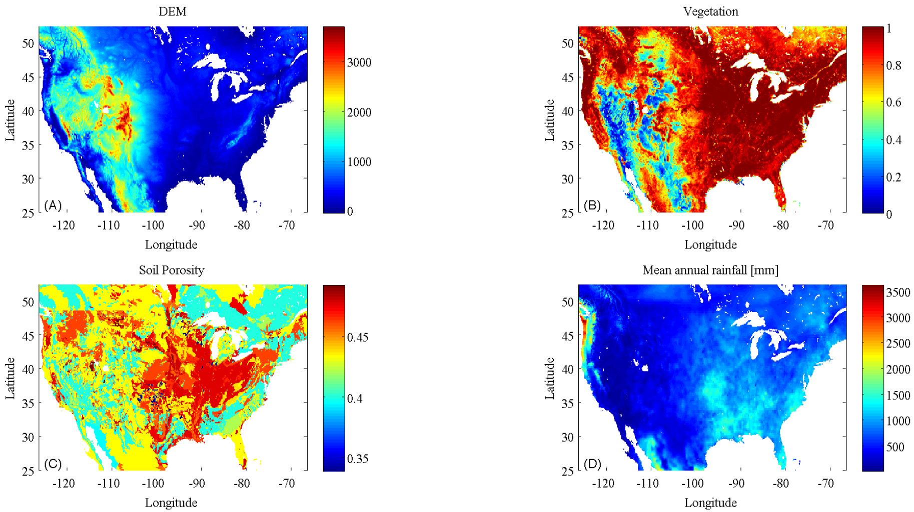

Fig. 4. (A) Digital Elevation Model (DEM) of North America (m a.s.l.), **(B)** fraction of the pixel covered by vegetation [–], **(C)** soil porosity [–] and **(D)** mean annual rainfall [mm yr^{-1}].

HESSD
9, 14129–14162, 2012

S. Manfreda et al.

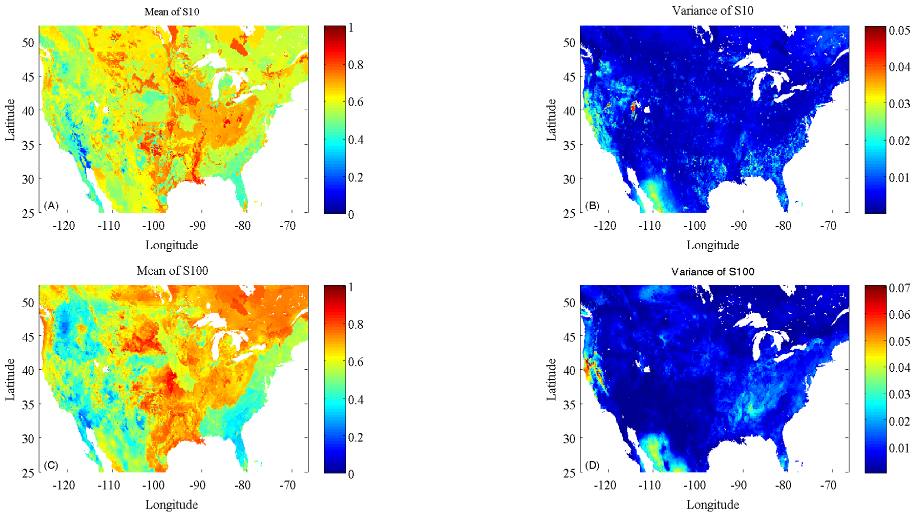

Fig. 5. Soil moisture statistics: mean value of relative soil moisture in the first 10 cm S10 **(A)**, variance of S10 **(B)**, mean value of the relative soil moisture in the first 100 cm S100 **(C)**, and variance of S100 **(D)**.

HESSD
9, 14129–14162, 2012

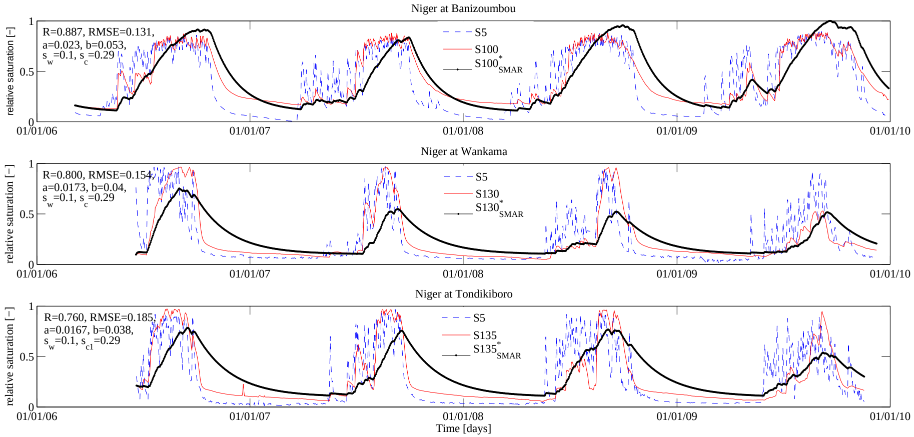

Fig. 6. Comparison between the relative saturation at 5 cm (S5) and the averaged value over 100, 130 and 135 cm of depth, and the filtered value ($S100^*_{SMAR}$ – green line) obtained with the SMAR for three sites located respectively at Banizoumbou, Wankama, and Tondikiboro. Results have been obtained assigning parameters defined on the physical characteristics of the study cases.

HESSD
9, 14129–14162, 2012

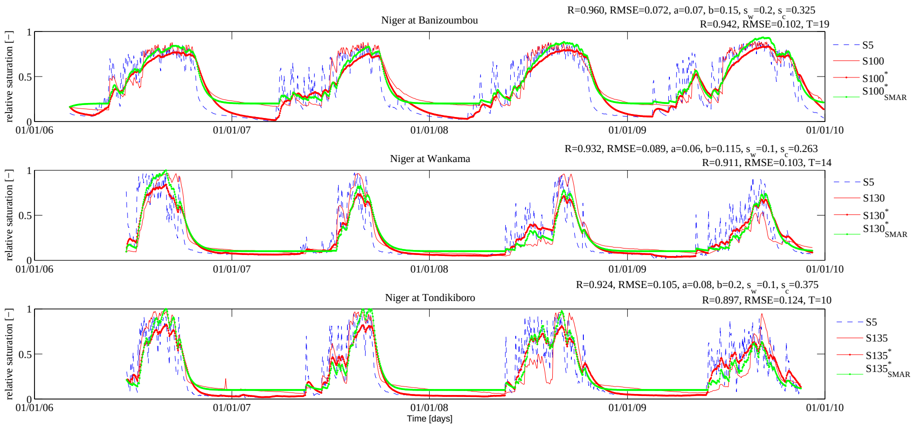

Fig. 7. Comparison between the relative saturation at 5 cm (S5) and the averaged value over 100, 130 and 135 cm of depth, the filtered value ($S100^{*}_{SMAR}$ – green line) obtained with the SMAR and the filtered value obtained with the exponential filter for three sites located respectively at Banizoumbou, Wankama, and Tondikiboro. Results describe the application of the SMAR and the exponential filter method where all parameters have been calibrated optimizing the RMSE.

HESSD
9, 14129–14162, 2012

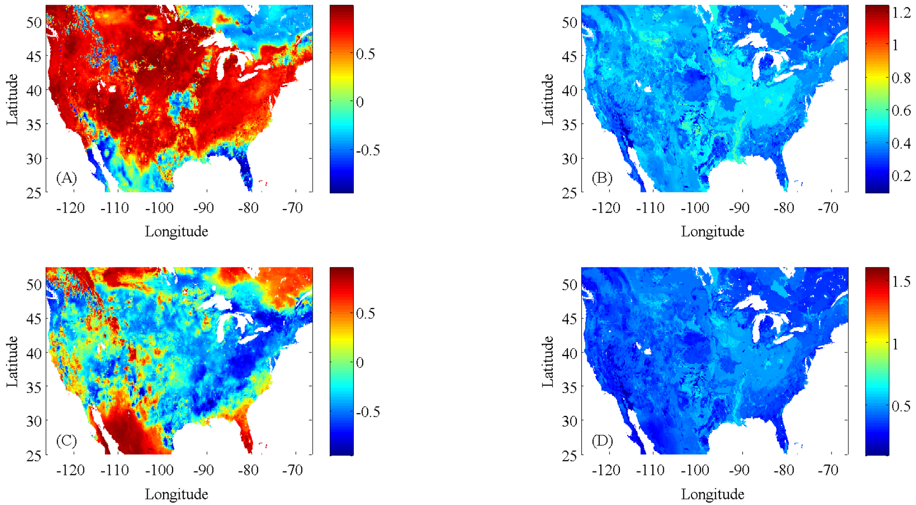

Fig. 8. Results of the calibration (**A** and **B**) and validation (**C** and **D**) of the exponential filter over the NLDAS domain. **(A)** Correlation coefficient between the filtered soil moisture and the simulated soil moisture in the first 100 cm at the daily time scale with the exponential filter for the first 6 months studied (October 1998–March 1999). Mean value of correlation obtained is $R = 0.463$ **(B)** RMSE obtained with the calibration procedure for the exponential filter (mean value of RMSE is equal 0.406). **(C)** Correlation coefficients obtained with the exponential filter for the period April 1999–September 1999 (observed mean value of $R = -0.068$). **(D)** RMSE with the exponential filter (mean value equal 0.411) for the period April 1999–September 1999.

HESSD
9, 14129–14162, 2012

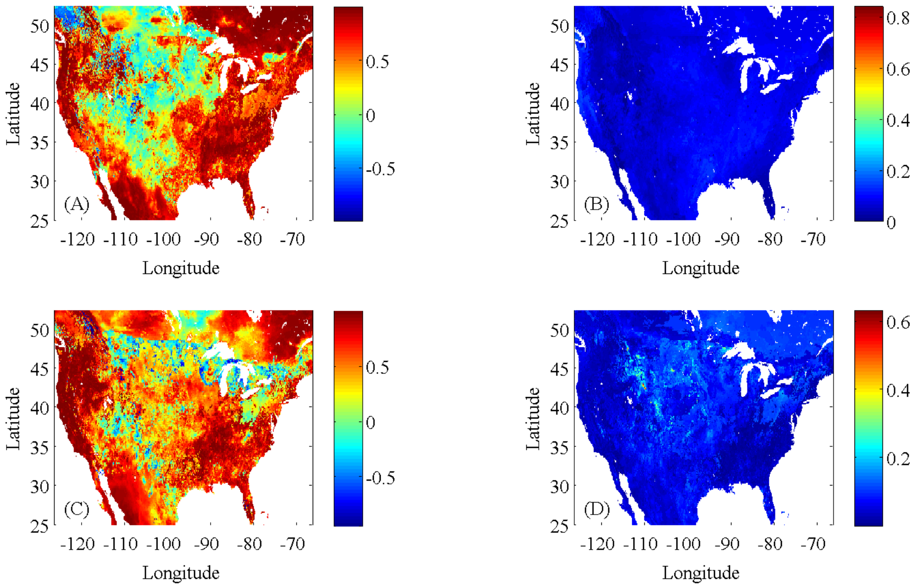

Fig. 9. Results of the calibration (**A** and **B**) and validation (**C** and **D**) of the SMAR over the NLDAS domain. **(A)** Correlation coefficient between the filtered soil moisture and the simulated soil moisture in the first 100 cm at the daily time scale with the SMAR for the first 6 months studied (October 1998–March 1999). Mean value of correlation obtained is $R = 0.6374$. **(B)** RMSE obtained with the calibration procedure for the SMAR (mean value of RMSE is equal 0.0773). **(C)** Correlation coefficients obtained with the SMAR for the period April 1999–September 1999 (observed mean value of $R = 0.5457$). **(D)** RMSE with the SMAR (mean value equal 0.0704) for the period April 1999–September 1999.

HESSD
9, 14129–14162, 2012
Predicting root-zone soil moisture using surface data
S. Manfreda et al.

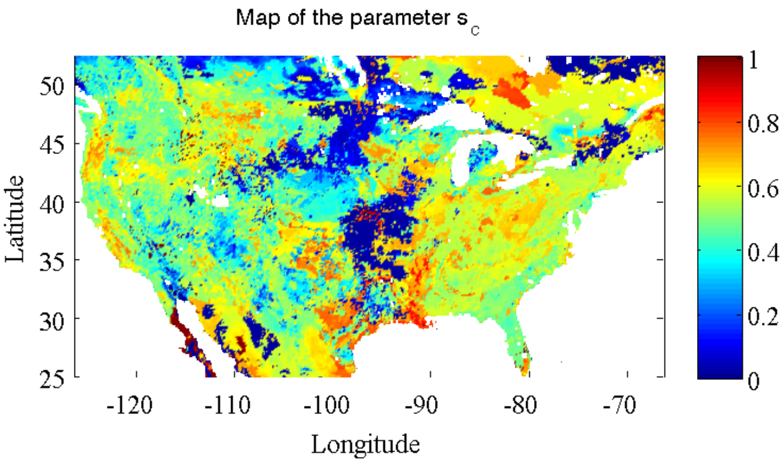

Fig. 10. Spatial distribution of the calibrated values of the parameter s_c over the NLDAS domain.

HESSD
9, 14129–14162, 2012

Predicting root-zone soil moisture using surface data

S. Manfreda et al.

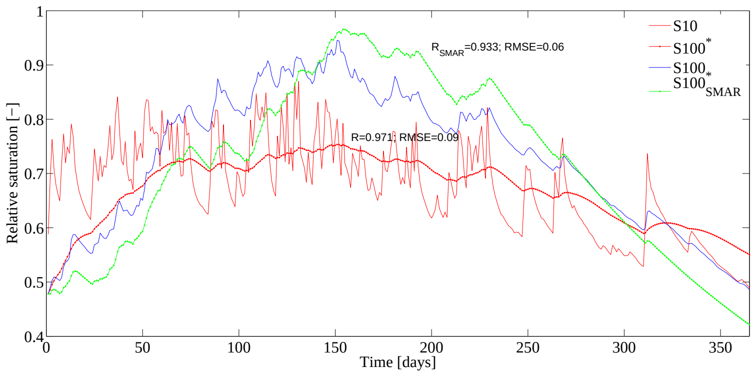

Fig. 11. Selected point comparison between the relative saturation at 10 cm and 100 cm depth and the filtered value ($S100^{*}_{SMAR}$ – green line) obtained with the SMAR (assuming the following parameters: $a = 0.006$, $b = 0.11$, $s_w = 0$, $s_{c1} = 0.665$) and with the exponential filter (assuming $T = 29$) ($S100^{*}$ – red line).

HESSD
9, 14129–14162, 2012

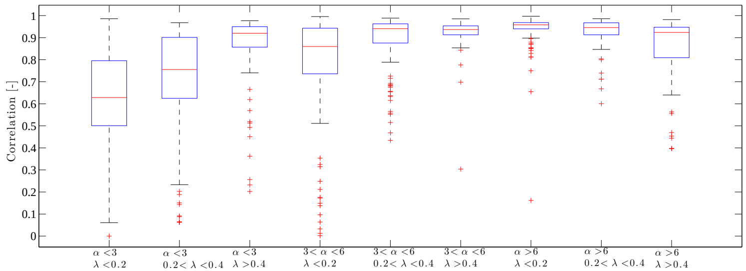

Fig. 12. Box-plot of the correlation between $S100^*_{SMAR}$ and S100 as a function of rainfall characteristics: mean rainfall rate (λ) and mean rainfall depth (α).

HESSD
9, 14129–14162, 2012

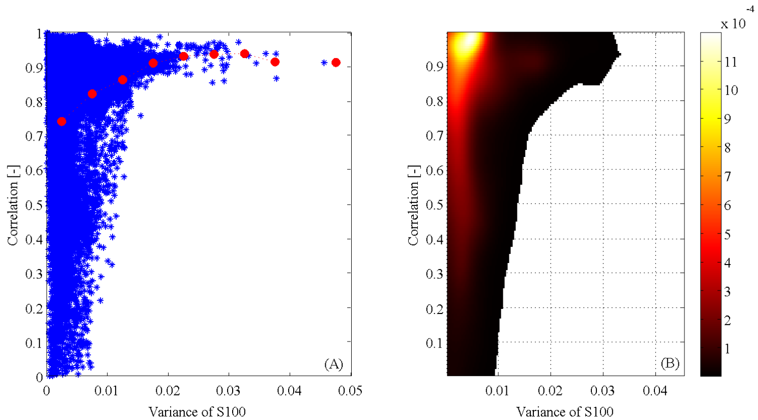

Fig. 13. (A) Values of correlation between $S100^{*}_{SMAR}$ and S100 as a function of the variance of S100. The red open circles describes mean of the observed cloud of data. **(B)** The 2-D histogram of the same data.

HESSD
9, 14129–14162, 2012

Predicting root-zone soil moisture using surface data

S. Manfreda et al.